

Supporting Information

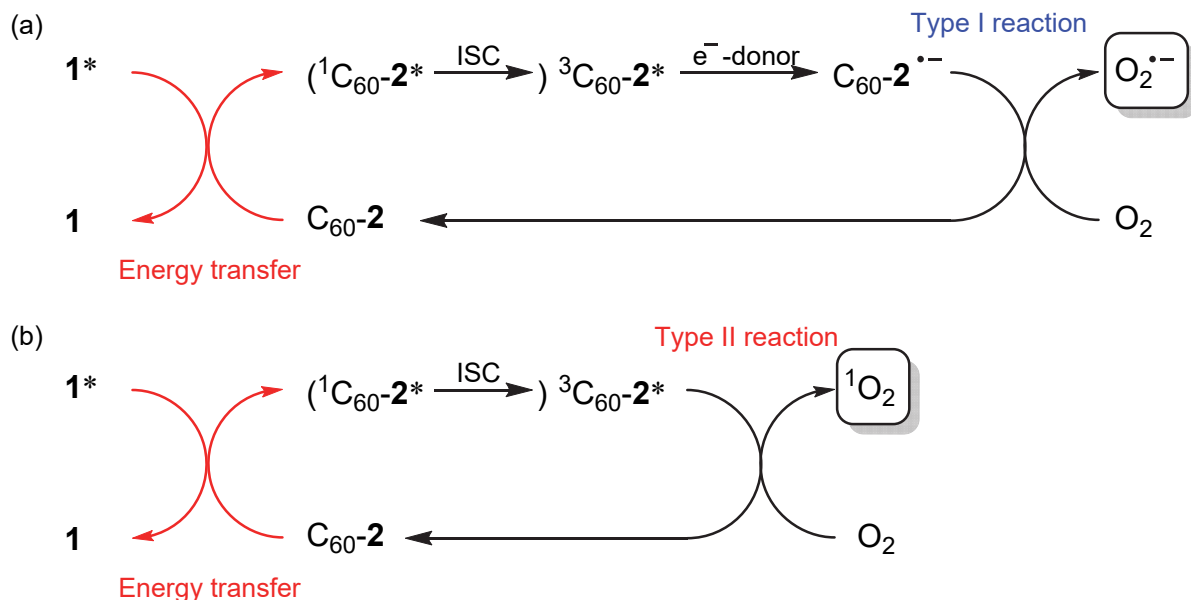
Improvement in photodynamic activity by porphyrin–fullerene composite system in lipid membrane

Kotaro Nishimura, Keita Yamana, Riku Kawasaki and Atsushi Ikeda *

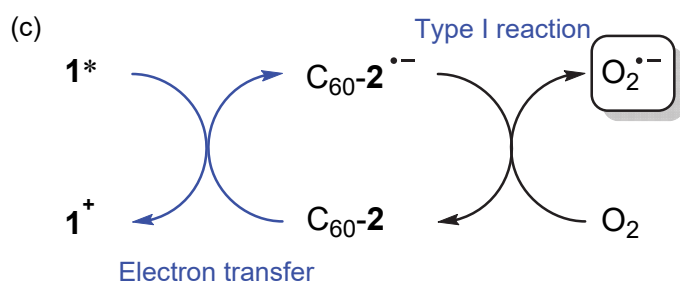
Applied Chemistry Program, Graduate School of Advanced Science and Engineering, Hiroshima University, 1-4-1 Kagamiyama, Higashi-Hiroshima 739-8527, Japan

Scheme S1. Energy or electron transfer mechanism from photoactivated **1** to C₆₀-**2**. If the triplet excited state of C₆₀-**2** (³C₆₀-**2**^{*}) is generated via energy transfer from photoactivated **1** to C₆₀-**2**, either O₂^{·-} or ¹O₂ can be produced by a Type I or Type II reaction between C₆₀-**2** and dissolved oxygen. Conversely, if the radical anion of C₆₀-**2** (C₆₀-**2**^{·-}) is generated via electron transfer from photoactivated **1** to C₆₀-**2**, only O₂^{·-} can be produced by a Type I reaction between C₆₀-**2**^{·-} and dissolved oxygen.

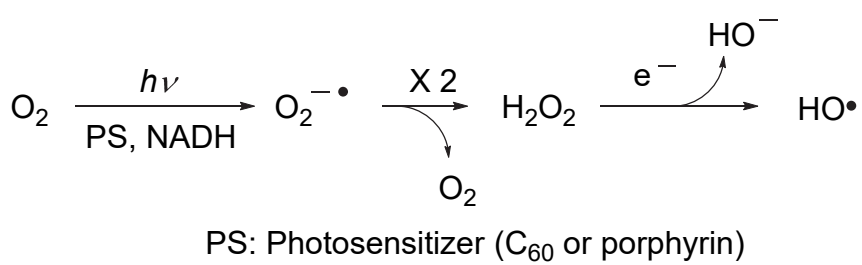
Energy transfer from porphyrin **1** to C₆₀-**2**



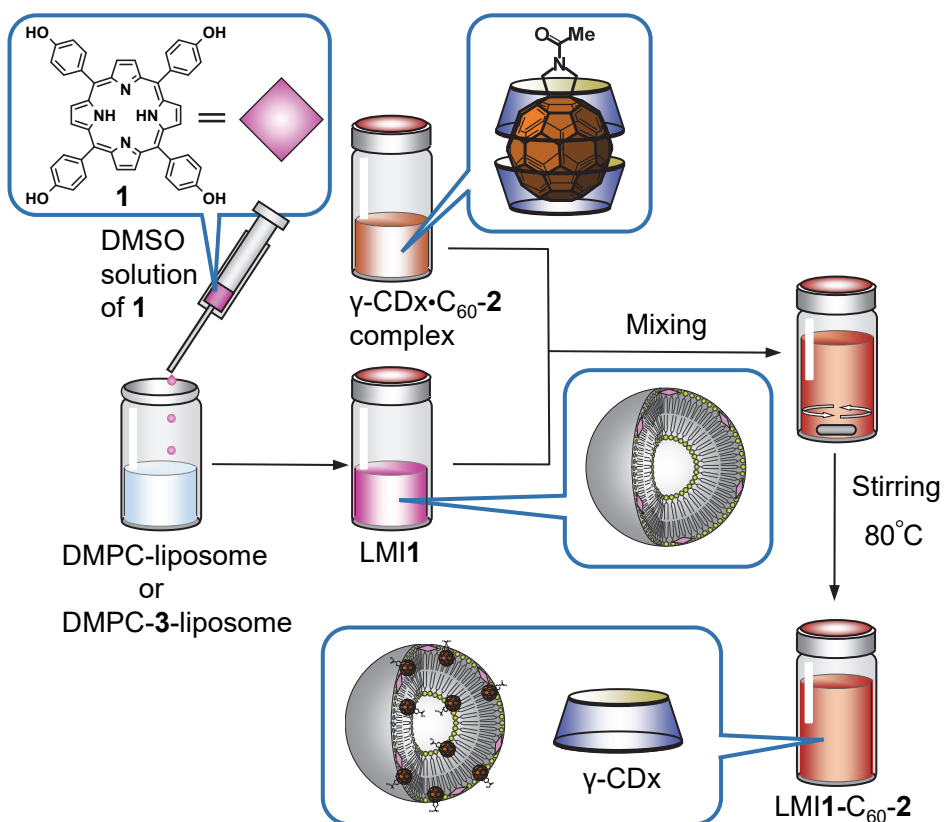
Electron transfer from porphyrin **1** to C₆₀-**2**



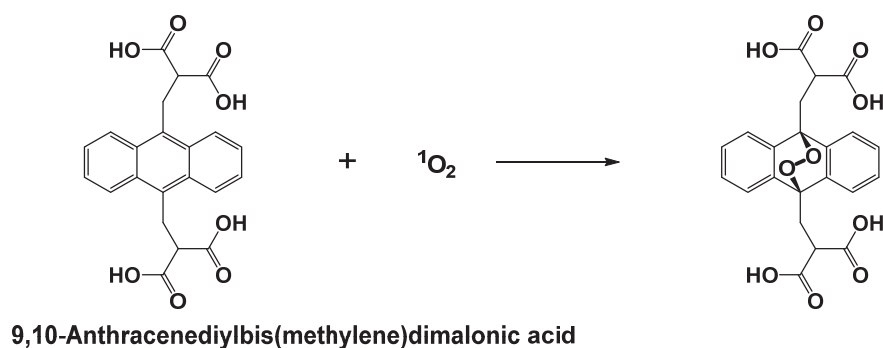
Scheme S2. Generation O₂^{·-} and then OH[·] from dissolved oxygen by photosensitizer²³



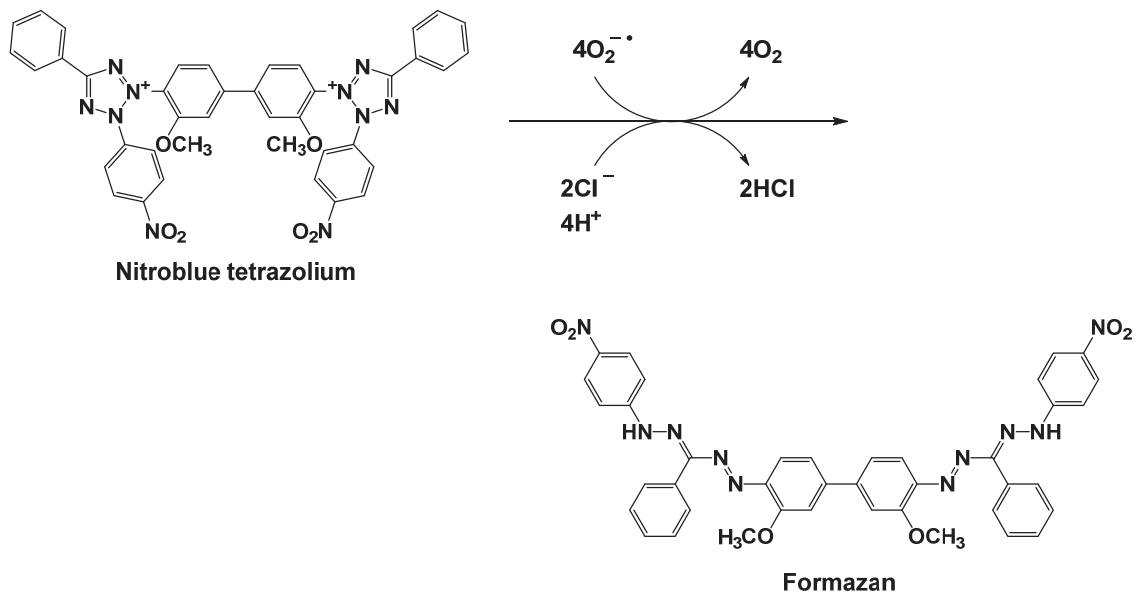
Scheme S3. Representation of the exchange method implemented for the preparation of LMI1–C₆₀–2 (γ -CDx = γ -cyclodextrin; LMI = lipid membrane–incorporated).



Scheme S4. Conversion of 9,10-anthracenediyl-bis(methylene)dimalonic acid to the corresponding endoperoxide as a result of reaction with singlet oxygen ($^1\text{O}_2$).



Scheme S5. Conversion of nitroblue tetrazolium to formazan as a result of reaction with superooxygen ($O_2^{\cdot-}$).



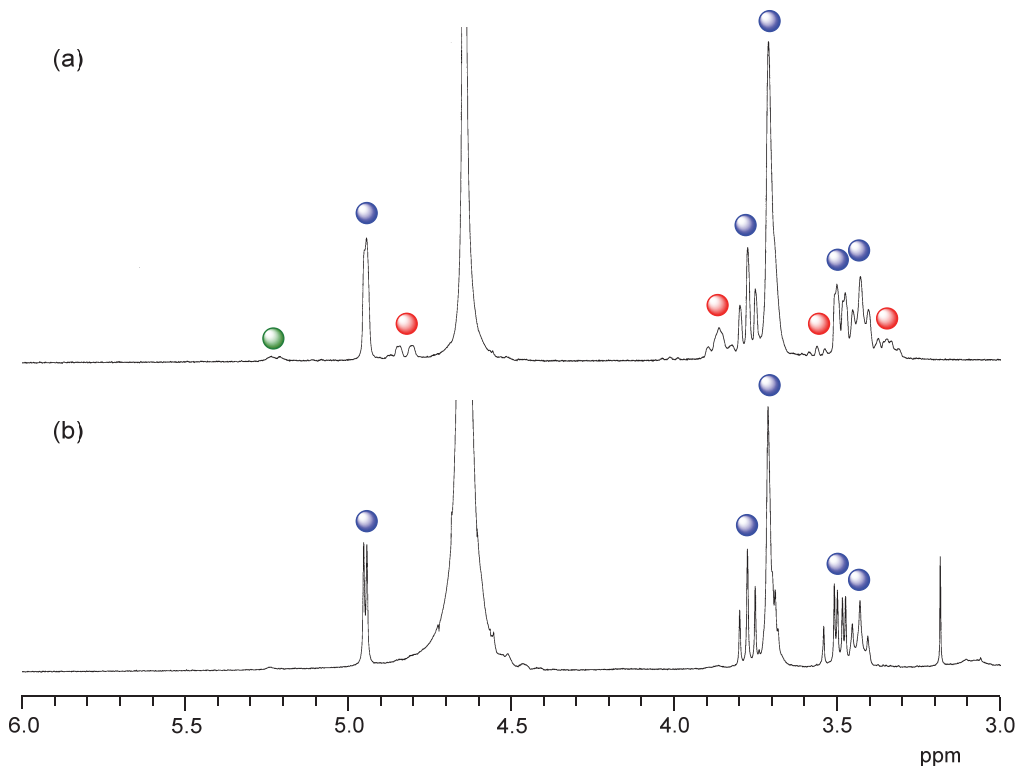


Fig. S1 Sections of the ^1H NMR spectra of the γ -cyclodextrin–C₆₀–**2** complex (a) before and (b) after the addition of the DMPC liposomes in D₂O. The blue circles indicate peaks due to free γ -cyclodextrin; the red circles indicate peaks due to γ -cyclodextrin in the γ -cyclodextrin–C₆₀–**2** complex; the green circle indicates the peak due to C₆₀–**2** in the γ -cyclodextrin–C₆₀–**2** complex. (a) [C₆₀–**2**] = 0.05 mM; [γ -cyclodextrin] = 0.7 mM; (b) [DMPC] = 1.0 mM; [C₆₀–**2**]/[DMPC] = 5.0 mol%; [DiD]/[DMPC] = 2.5 mol%.

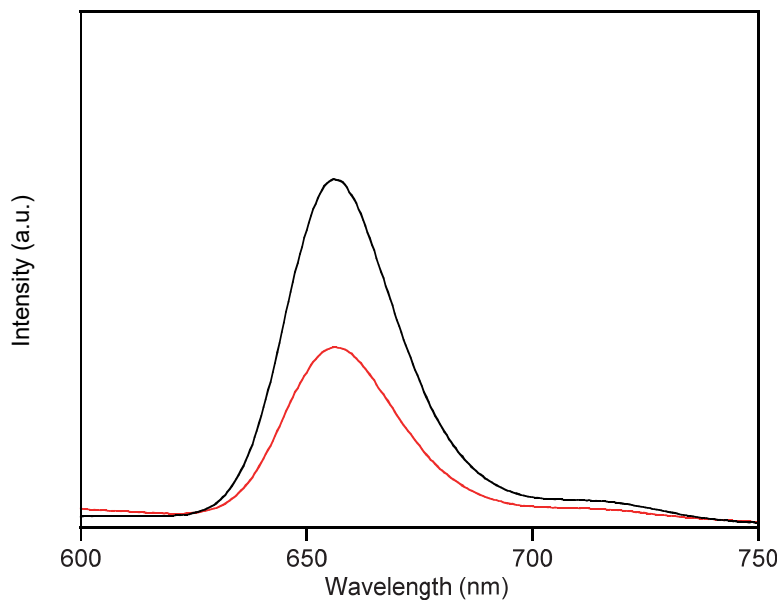


Fig. S2 Fluorescence spectra (λ_{ex} : 570 nm) of LMI1 (black line) and LMI1–C₆₀–**2** (red line) ([DMPC] = 0.1 mM; [1]/[DMPC] = 2.5 mol%; [C₆₀–**2**]/[DMPC] = 5.0 mol%) in water.

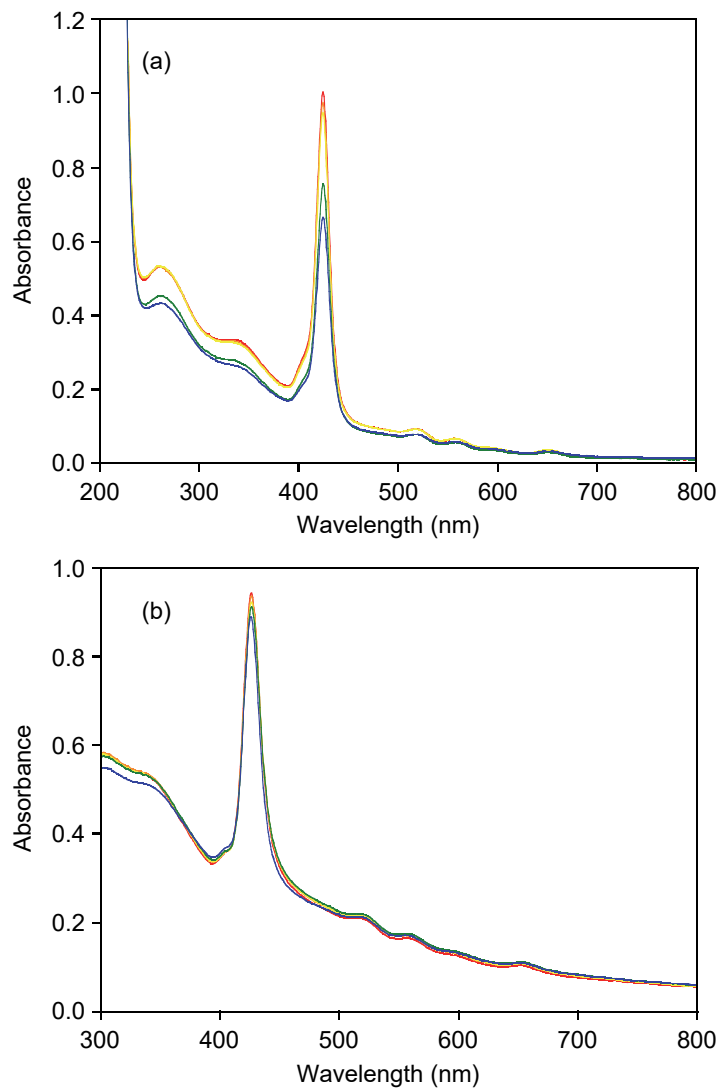


Fig. S3 UV–Vis absorption spectra of LMI1–C₆₀–2 (a) in water after incubation times of 0 (red), 1 (orange), 3 (yellow), 5 (green), and 7 (blue) days and (b) in blood serum after incubation times of 0 (red), 2 (orange), 4 (yellow), 6 (green), and 24 (blue) hours at 37 °C using a 1-cm cell ([DMPC] = 0.1 mM; [1] = 2.5 μM; [C₆₀–2] = 5.0 μM).

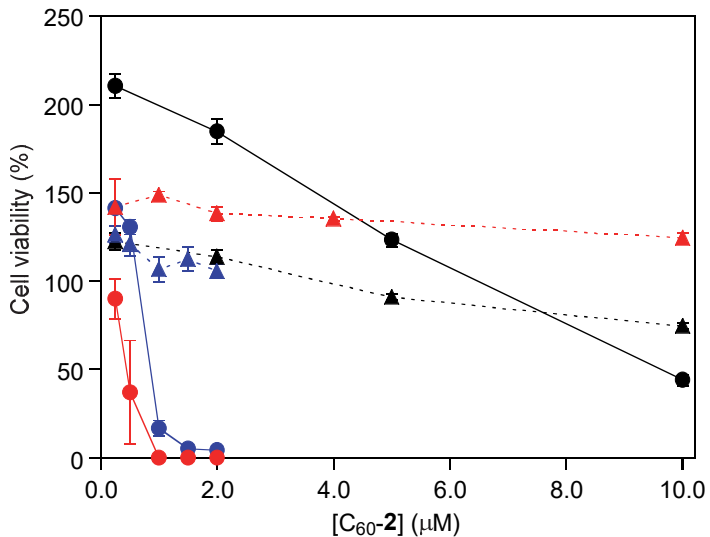


Fig. S4 Cell viability of Colon26 cells treated with LMIC₆₀-2 (black), LMI1-C₆₀-2 (red), and LMI1+LMIC₆₀-2 mixture (blue) in the dark (triangles and dashed lines) and after photoirradiation at 610–740 nm for 30 min (circles and solid lines) at concentrations of C₆₀-2 ranging from 0.25 to 10.0 μM. The cell viability was evaluated 24 h after treatment using the WST-8 method. The error bars represent the mean ± standard deviation for *n* = 3.

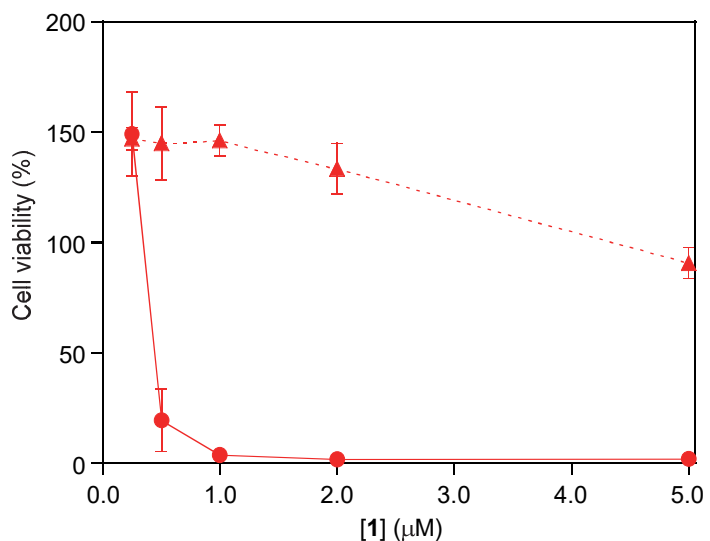


Fig. S5 Cell viability of L929 cells treated with LMI1-C₆₀-2 in the dark (triangles and dashed lines) and after photoirradiation at 610–740 nm for 30 min (circles and solid lines) at concentrations of C₆₀-2 ranging from 0.25 to 5.0 μM. The cell viability was evaluated 24 h after treatment using the WST-8 method. The error bars represent the mean ± standard deviation for *n* = 3.

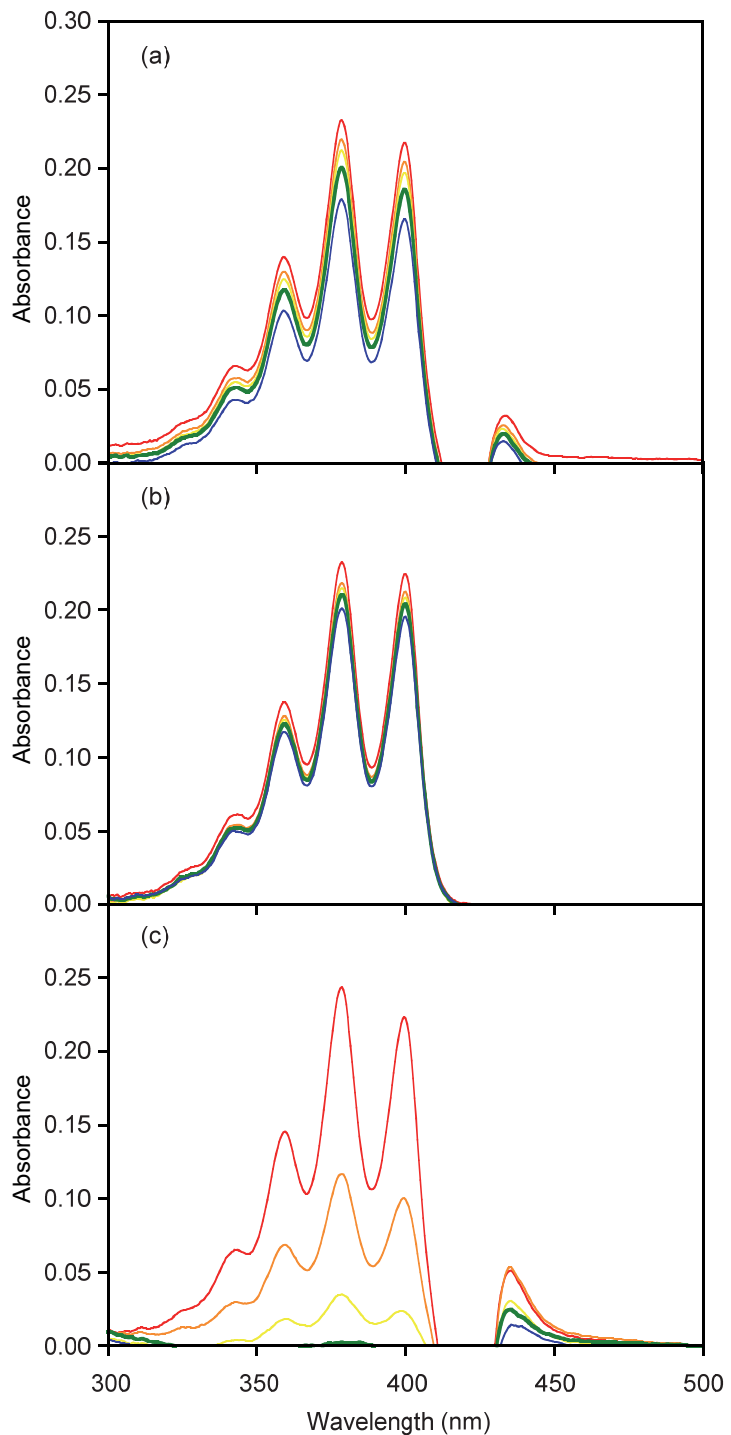


Fig. S6 Time-dependent bleaching of 9,10-anthracenediyl-bis(methylene)dimalic acid (ABDA) caused by the generation of singlet oxygen by (a) LMI1, (b) LMIC₆₀-2, and (c) LMI1-C₆₀-2, upon photoirradiation ($\lambda > 620$ nm, 15 mW cm⁻²) for 0 (red line), 7.5 (orange line), 15 (yellow line), 30 (green line), and 60 (blue line) min. A dimethyl sulfoxide solution of ABDA was injected into aqueous solutions of the liposomes. The absorption spectra were obtained by subtracting the absorption of LMI1, LMIC₆₀-2, and LMI1-C₆₀-2, respectively. [DMPC] = 0.1 mM, [1] = 0 or 2.5 μ M, [C₆₀-2] = 0 or 5.0 μ M, and [ABDA] = 25 μ M; 1-cm cell. The experiments were conducted under an oxygen atmosphere at 25 °C.

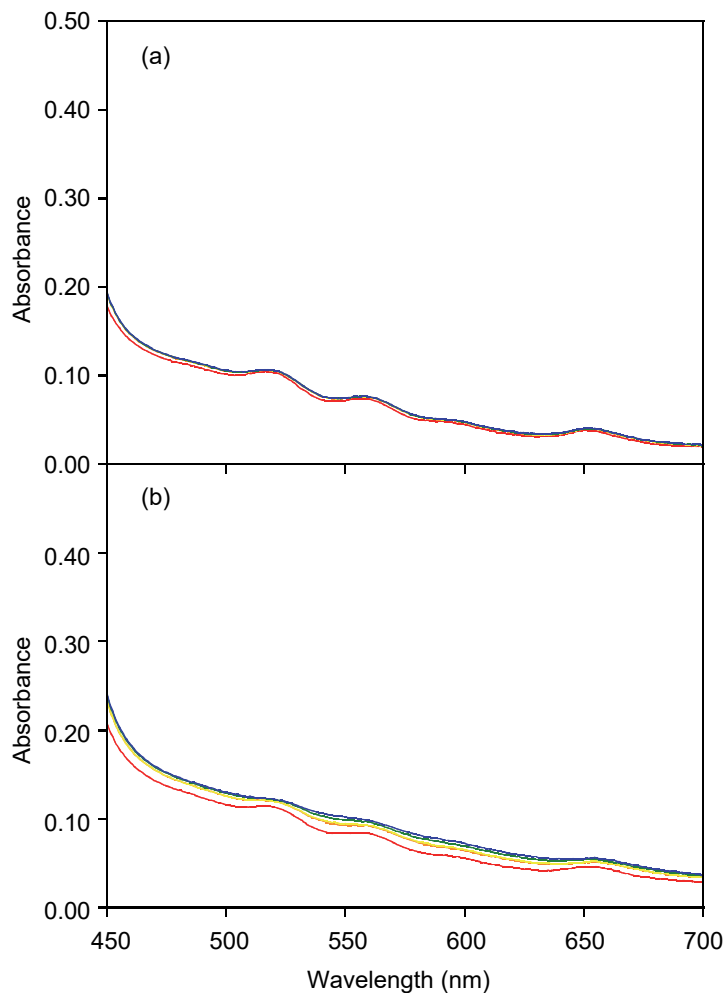


Fig. S7 Changes in the UV–Vis absorption of formazan generated by the reduction of NBT in the presence of LMI1–C₆₀–**2** in (a) the absence and (b) the presence of NADH, after photoirradiation at a wavelength greater than 620 nm for 0 (red line), 7.5 (orange line), 15 (yellow line), 30 (green line), and 60 (blue line) min. [DMPC] = 0.1 mM, [1] = 0 or 2.5 μ M, [C₆₀–**2**] = 0 or 5.0 μ M, [NBT] = 0.20 mM, and [NADH] = 0 or 0.50 mM; 1-cm cell. The experiments were conducted under an oxygen atmosphere at 25 °C.

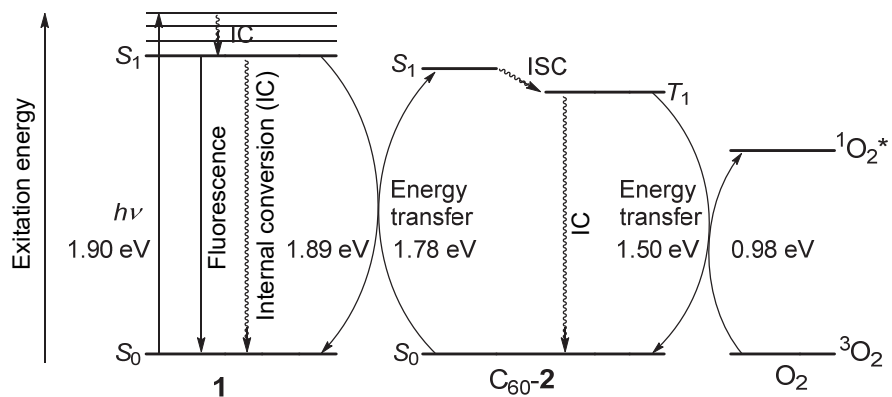


Fig. S8 Schematic illustrations of Jablonski diagrams in LMI1–C₆₀-2 (The energy potential ($S_0 \rightarrow S_1$) of C₆₀-2 was determined using the wavelength of maximum fluorescent emission of γ -cyclodextrin–C₆₀-2 complex.²⁸ The energy potential ($T_1 \rightarrow S_0$) of C₆₀-2 was determined from wavelength of maximum phosphorescence emission of *N*-methyl fulleropyrrolidine in methylcyclohexane, which was reported in Ref. S1 and S2, because the phosphorescence of C₆₀-2 has not reported.).

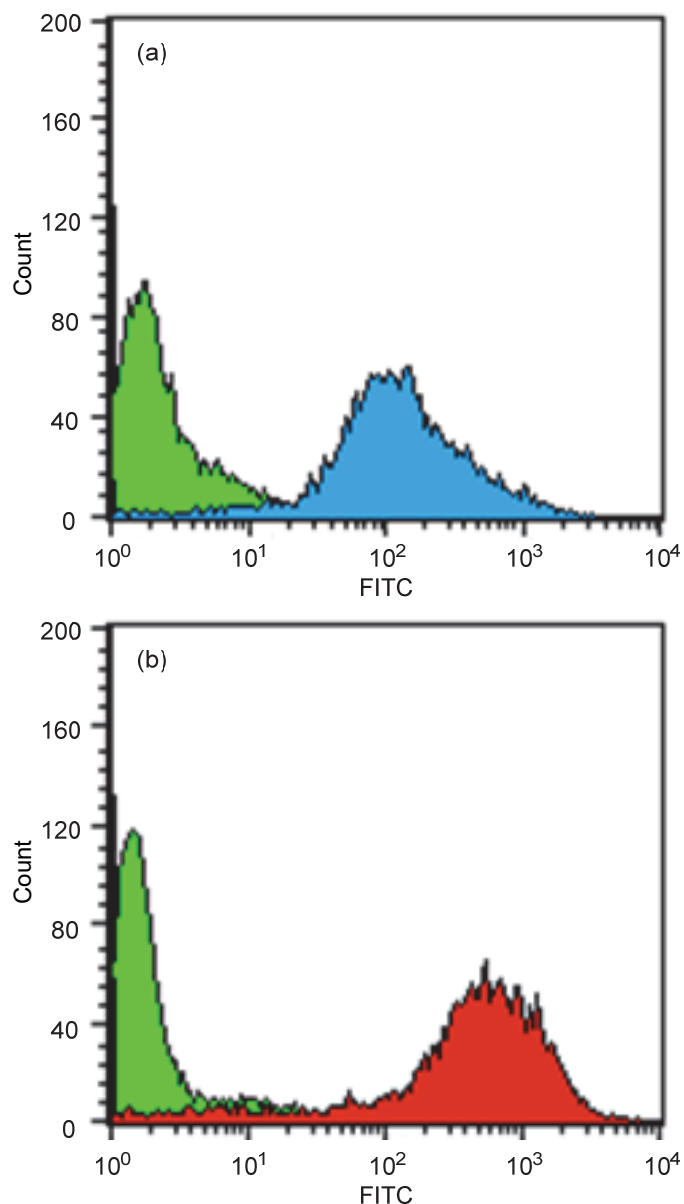


Fig. S9 Flow cytometry analysis for the detection of LMI1–C₆₀–**2** in (a) Colon26 (blue) and (b) HeLa (red) cells treated with LMI1–C₆₀–**2** ([DMPC] = 0.04 mM, [1] = 1.0 μ M, [C₆₀–**2**] = 2.0 μ M) and control (green; [DMPC] = [1] = [C₆₀–**2**] = 0 mM).

References

- S1 R. M. Williams, J. M. Zwier and J. W. Verhoeven, *J. Am. Chem. Soc.*, 1995, **117**, 4093–4099.
- S2 C. Luo, M. Fujitsuka, A. Watanabe, O. Ito, L. Gan, Y. Huang and C.-H. Huang, *J. Chem. Soc., Faraday Trans.*, 1998, **94**, 527–532.